Fate of the Nitrilotriacetic acid -Fe(III) complex during photodegradation and biodegradation by Rhodococcus rhodochrous.

Andrei Bunescu, Pascale Pascale Besse, P. Besse-Hoggan Besse-Hoggan, Martine Sancelme, Gilles Mailhot, A.M. Delort

Fate of the Nitrilotriacetic Acid-Fe(III) Complex during Photodegradation and Biodegradation by *Rhodococcus rhodochrous*

Andrei Bunescu,[1,2,3] Pascale Besse-Hoggan,[1] Martine Sancelme,[1] Gilles Mailhot,[2] and Anne-Marie Delort[1]*

Laboratoire de Synthèse Et Etude de Systèmes à Intérêt Biologique, UMR 6504 CNRS-Université Blaise Pascal, 63177 Aubière Cedex, France[1]; Laboratoire de Photochimie Moléculaire et Macromoléculaire, UMR 6505 CNRS-Université Blaise Pascal, 63177 Aubière Cedex, France[2]; and Laboratory of Organic Chemistry, State University of Moldova, 60 A. Mateevici Str., Chisinau MD-2009, Republic of Moldova[3]

Aminopolycarboxylic acids are ubiquitous in natural waters and wastewaters. They have the ability to form very stable water-soluble complexes with many metallic di- or trivalent ions. The iron complex nitrilotriacetic acid-Fe(III) (FeNTA) has been previously shown to increase drastically the rate of photo- and biodegradation of 2-aminobenzothiazole, an organic pollutant, by *Rhodococcus rhodochrous*. For this paper, the fate of FeNTA was investigated during these degradation processes. First, it was shown, using in situ ^{1}H nuclear magnetic resonance, that the complex FeNTA was biodegraded by *Rhodococcus rhodochrous* cells, but the ligand (NTA) alone was not. This result indicates that FeNTA was transported and biotransformed inside the cell. The same products, including iminodiacetic acid, glycine, and formate, were obtained during the photo- and biodegradation processes of FeNTA, likely because they both involve oxidoreduction mechanisms. When the results of the different experiments are compared, the soluble iron, measured by spectrophotometry, was decreasing when microbial cells were present. About 20% of the initial iron was found inside the cells. These results allowed us to propose detailed mechanistic schemes for FeNTA degradation by solar light and by *R. rhodochrous*.

Nitrilotriacetic acid (NTA) (Fig. 1) belongs to the wide family of so-called aminopolycarboxylic acids (APCAs) containing several carboxylate groups bound to one or more nitrogen atoms (for reviews, see references 4 and 9). These APCAs have the ability to form very stable water-soluble complexes with many metallic di- or trivalent ions. Some of these APCAs are naturally synthesized by plants or microorganisms and are involved in the uptake of metals by these organisms. Due to their remarkable complexation properties, synthetic APCAs have been used for domestic and industrial applications to control the solubility and precipitation of metallic ions. More specifically, NTA was used as a chelating agent and as a substitute for phosphates in detergents. In 1999, about 20,000 tons of NTA was used in Europe. As a result of this massive use, NTA can be rejected in the environment. Actually, NTA is rarely encountered in soils, sediments, natural waters, and wastewater treatment plants, suggesting that it is efficiently eliminated by photodegradation and biodegradation mechanisms.

The APCAs, like NTA, do not absorb solar light, and as a consequence, their photolysis is negligible. However, one of the ways of APCA degradation in the natural environment comes from the fact that they are strong complexing agents. For example, the iron complex nitrilotriacetic acid-Fe(III) (FeNTA), usually considered a model for iron complexes present in natural organic matter and in water, presents an absorption band up to 400 nm (2). Therefore, this complex can absorb solar light and undergo an efficient photoredox process. This intramolecular photoredox process leads to the reduction of the metal and the oxidation of the ligand NTA. The quantum yields of FeNTA disappearance at 365 nm at pH 4.0 and 7.0 are 0.18 and 0.09, respectively. The major photoproducts observed are Fe(II), iminodiacetic acid (IDA), formaldehyde, and CO_2 (see Fig. 1) (2). Moreover, during this process, radical species are formed and are capable of degrading organic compounds present in an aqueous solution (1). Two main radicals have been identified: (i) hydroxyl radical HO$^\bullet$ formed through a Fenton process (H_2O_2 is formed during a photochemical process) or directly at a shorter wavelength (λ, ~310 to 320 nm) and (ii) carbonate radical $CO_3^{\bullet -}$ formed at a shorter wavelength. In the latter case, there is an electron transfer from the OH^- or H_2O ligand to Fe(III), leading to the formation of HO$^\bullet$. The hydroxyl radical is expected to abstract hydrogen from the methylene carboxylate group by a reaction in cage. The so-formed radical can then react with oxygen and by rearrangement lead to the carbonate radical anion (1).

Concerning biodegradation, only a few bacterial isolates have been identified as being able to transform NTA. All are gram-negative and aerobic bacteria. Strains from the two main genera *Chelatobacter* and *Chelatococcus*, strictly aerobic members of the alpha-2 subgroup of *Proteobacteria*, and an aerobic strain related to the *Xanthomonas* group of the gamma subgroup of *Proteobacteria* have been reported (4). The metabolic pathways involved in NTA biodegradation have been studied in detail, particularly with the strains *Chelatobacter heintzii* (*Aminobacter aminovorans*) and *Chelatococcus asaccharovorans* (9). Two cytoplasmic enzymatic complexes transform NTA into IDA and glyoxylate, whose struc-

* Corresponding author. Mailing address: Laboratoire de Synthèse Et Etude de Systèmes à Intérêt Biologique, UMR 6504 CNRS-Université Blaise Pascal, 63177 Aubière Cedex, France. Phone: 33 4 73 40 77 14. Fax: 33 4 73 40 77 17. E-mail: A-Marie.DELORT@univ-bpclermont.fr.

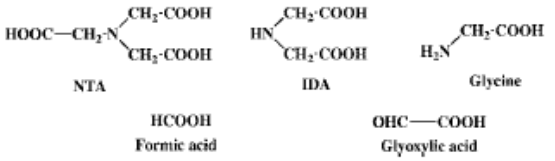

FIG. 1. Chemical structures of NTA, IDA, glycine, formic acid, and glyoxylic acid.

tures are shown in Fig. 1. The first system is a monooxygenase/$NADH_2$:flavin mononucleotide (FMN) oxidoreductase enzyme which has been purified and characterized; it uses oxygen from the air. The second system is an oxygen-independent NTA dehydrogenase isolated from a denitrifying NTA-degrading bacterium. IDA can be cleaved into glycine and glyoxylate (Fig. 1) via a membrane-bound IDA dehydrogenase. Glyoxylate and glycine are then easily integrated into the central metabolism.

A very important point concerning APCA complexes is their metal speciation, as it can influence both their transport in the cell and their biodegradability. Considering whole cells, it is difficult to study the importance of this factor, and data reported in the literature are quite contradictory. Obviously, it might depend on the organism. For instance, in *C. heintzii*, all metallic NTA complexes with Ca^{2+}, Mn^{2+}, Mg^{2+}, Zn^{2+}, Cd^{2+}, and Fe^{3+} as well as free NTA are degraded but NiNTA is not (9). Also, the transport of NTA in the cell is not yet established; it is not known if it is transported as a complex or in its free form. The study of isolated enzymes showed some specificities; for instance, the NTA-monooxygenase/$NADH_2$:FMN oxidoreductase accepts MgNTA, CoNTA, ZnNTA, MnNTA, and FeNTA as substrates, while the NTA dehydrogenase can transform only free NTA (9).

In a previous paper (5), we showed that the iron complex FeNTA greatly increased the degradation rate of the organic pollutant 2-aminobenzothiazole (ABT), both under sunlight irradiation and during incubation with the strain *Rhodococcus rhodochrous* OBT18. This strain was isolated from a wastewater treatment plant of Bayer industry in Belgium (7) and is known to degrade several benzothiazole derivatives (3, 11). This activation effect of ABT disappearance was also observed when photodegradation and biodegradation processes were combined. This phenomenon was very intriguing and has not been described to date. The objective of the present work was to investigate further the fate of the iron complex FeNTA during these various processes (photodegradation, biodegradation, and combined techniques) in order to provide evidence for the accelerating effect of FeNTA. To our knowledge, no isolate belonging to the genus *Rhodococcus* or any gram-positive bacterium has been shown to transform NTA. Also, the phototransformation of FeNTA was not studied before in the presence of microbial cells. Therefore, the transformation of the FeNTA complex and the NTA ligand alone was studied in detail using in situ ^1H nuclear magnetic resonance (NMR), and the localization of iron was investigated further using complexometric methods.

MATERIALS AND METHODS

All the experiments were repeated two times, and three samples were taken for each time of incubation. Each value reported on the graphs in the figures corresponds to the average of three measurements.

Chemicals. ABT, NTA, IDA, EDTA, hydroxylamine chlorhydrate, and ferrozine [3-(2-pyridyl)-5,6-diphenyl-1,2,4-triazine-4,4′-disulfonic acid, sodium salt, 97%] were purchased from Aldrich. Glycine and Fe(III) perchlorate [$Fe(ClO_4)_3$, $9H_2O$] were purchased from Fluka. The perchlorate is used as a counter-anion because it is not photosensitive and it is not an oxidant, unlike the chlorate anion that can strongly contribute to the oxidation of benzothiazole and interfere with our results. Tetradeuterated sodium trimethylsilylpropionate (TSP-d_4) was purchased from Eurisotop (Saint Aubin, France).

Preparation of the FeNTA (2 mM) solution. To a 100-ml aqueous solution containing 4 mM NTA at a pH of 4.0 was added, under stirring, 100 ml of a freshly prepared solution of 4 mM $Fe(ClO_4)_3$. This mixture was stirred for 1 h, and the pH was adjusted to 4.0 with 1 N NaOH. The total complexation of the iron was controlled by UV-visible spectrophotometry ($\varepsilon_{260\ nm}$ = 6,000 M^{-1} cm^{-1}). The analysis gave evidence for a 1:1 stoichiometry. The pH of the FeNTA solution was adjusted to 7.0 with 1 N NaOH just before the experiment.

Growth conditions and incubation with xenobiotic compounds. *Rhodococcus rhodochrous* OBT18 was grown in 100-ml portions of Trypticase soy broth (bioMérieux, Marcy l'Etoile, France) in 500-ml Erlenmeyer flasks incubated at 27°C and 200 rpm. The cells (300 ml of the culture medium) were harvested after 24 h of culture and centrifuged at 8,000 rpm for 15 min at 4°C. The bacterial pellet was washed first with an NaCl solution (8 g $liter^{-1}$) and then with Volvic mineral water to keep a constant mineral composition. The resting cells (600 mg dry weight in 100 ml Volvic water) were incubated with ABT (0.5 mM) and/or FeNTA (1 mM) in 500-ml Erlenmeyer flasks (in borosilicate or brown glass) at 27°C under agitation (200 rpm) and light irradiation. The initial ABT solution at 1.0 mM was prepared in Volvic mineral water. Samples (three, 1 ml each) were regularly taken directly from the incubation medium and centrifuged at 12,000 rpm for 5 min. One milliliter of supernatant was directly used for iron measurement, and the other 2 ml was frozen until analyses by high-performance liquid chromatography (HPLC) or NMR. The controls consisted of preparations incubated under the same conditions without the cells or without the substrate.

Incubator. The incubator was equipped with seven TLD Philips fluorescent tubes of 15 W, emitting within the wavelength range of 300 to 500 nm (polychromatic irradiation) with a maximum of emission at 360 nm. The irradiated or incubated media were placed in 500-ml Erlenmeyer flasks at 27°C under agitation (200 rpm) to maintain the homogeneity and the oxygenation of the suspension. The polychromatic photon flux was measured and controlled with a Testo 545 luxmeter.

Analytical methods (HPLC and NMR). (i) HPLC analyses. HPLC analyses were performed using a Waters 510 chromatograph fitted with a Waters UV-DAD 996 detector and a reversed-phase column (Interchrom Nucleosil C_8, 5 μm, 250 by 4.6 mm; Interchim) at room temperature. The mobile phase was acetonitrile-water (25/75, vol/vol) with a flow rate of 1 ml/min and a λ range from 200 to 400 nm.

(ii) ^1H NMR spectroscopy. All NMR spectra were recorded with a Bruker Avance 500 spectrometer at 298 K by using a 5-mm triple-tuned ^1H-^{13}C-^{15}N probe equipped with a z-gradient coil. Water resonance was suppressed by using the classical double pulsed-field gradient echo sequence WATERGATE. A total of 128 scans were collected (relaxation delay, 1 s; acquisition time, 4.67 s; spectral window, 7,002 Hz; 65,536 data points). A 1-Hz line-broadening procedure was applied before Fourier transformation, and a baseline correction was performed on spectra before integration with Bruker software. TSP-d_4 was used as an internal reference for chemical shift (0 ppm) and for quantification of the degradation products. To 540 μl of supernatant was added 60 μl of a 5 mM TSP-d_4 solution in D_2O. The experimental error is estimated to be less than 10% for the NMR experiments.

(iii) Sample preparation for NMR. Iron was removed from the samples by precipitation as follows. To 440 μl of supernatant was added 60 μl of a 5 mM TSP-d_4 solution in D_2O and 100 μl of 1 M NaOH solution (in D_2O) to obtain a pH around 13 for the iron precipitation. The mixture was stirred regularly for 1 h 30 min. The sample was then centrifuged at 12,500 × *g* for 3 min. The pH of 550 μl of the supernatant was adjusted to 7 with HCl at concentrations of 1 M (90 μl) and 0.01 M (solutions prepared in D_2O).

Titration by NMR of carboxylic acids (NTA and IDA) and glycine. A solution of NTA, IDA, and glycine (1.0 mM of each compound) was prepared in D_2O with TSP-d_4. The pH of the mixture was adjusted from 1 to 13 in steps of one unit by adding 1 M HCl and 1 M NaOH. At each pH, a ^1H NMR spectrum was recorded to determine the chemical shift of each compound. A titration curve was then plotted with the chemical shift against pH (Fig. 2). In the pH range from 4 to 8, the signals corresponding to the three compounds were well separated. Therefore, the pH of all samples was adjusted to around 7 before analysis.

Iron titration (according to Stookey [14]). The total iron concentration was determined after the reduction of Fe(III) species with a solution of hydroxylamine chlorhydrate (3 mM) (dissolution in a 500-ml flask of 104.25 mg of the salt

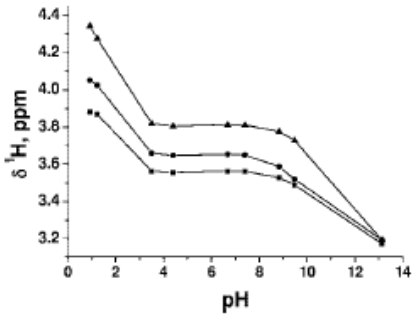

FIG. 2. Titration curves of the ^{1}H NMR chemical shifts of NTA (▲), IDA (●), and glycine (■) versus pH.

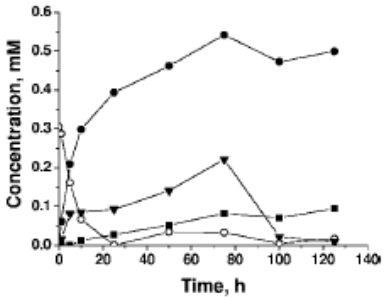

FIG. 4. Time courses of the concentrations of NTA (○), IDA (●), glycine (■), and formate (▼) under irradiation of a solution of FeNTA (1.0 mM) measured by ^{1}H NMR after iron precipitation.

into 200 ml of 32% HCl complete with distilled water). Ferrozine forms a strong-colored complex with Fe(II). To a 5-ml flask was added 0.25 ml of the sample, 1.5 ml water, and 0.5 ml of hydroxylamine solution (3 mM). After stirring vigorously and waiting for 10 min, 0.5 ml ferrozine (0.02 M), 1 ml of 0.1 N ammonium acetate buffer, and water to complete the mixture to 5 ml was added. After stirring, the optical density was measured at a λ of 562 nm. The experimental error for iron titration is less than 5%.

Titration of iron in the different compartments (solution, adsorbed on the cells, and inside the cells). At the end of the experiment with FeNTA (1.0 mM) and ABT (0.5 mM) without light (after 150 h of incubation), 30 ml of the solution was sampled and separated into two fractions. The first fraction (5 ml) was diluted with 10 ml of 0.1 M acetate buffer, mechanically ruptured under 2 Kbar of pressure, and centrifuged at 12,000 rpm for 15 min, and the total iron was titrated in the supernatant after dilution in a 50-ml flask with 0.1 M acetate buffer (A_i) and in the pellet after resuspension in a 50-ml flask with 0.1 M HCl (A_f). The sum of the two concentrations ($A_i + A_f$) gave the total amount of iron. The second fraction (25 ml) was centrifuged at 12,000 rpm for 15 min, and titration of the soluble iron in the supernatant (B_0) was performed. The pellet was then washed with 10 ml of a solution of EDTA (2.0 mM), prepared previously in 0.1 M acetate buffer. After centrifugation, the iron concentration in the supernatant (B_1) was determined. This step with EDTA was repeated three more times. The sum ($B_1 + B_2 + B_3 + B_4$) gave the concentration of the iron absorbed at the surface of the cells. The pellet was then resuspended in 10 ml of 0.1 M acetate buffer, and the cells were mechanically ruptured under 2 Kbar of pressure. After centrifugation at 12,000 rpm for 15 min, iron titration was carried out in the supernatant after dilution in a 25-ml flask with acetate buffer (B_i) and in the pellet after resuspension in a 25-ml flask with 0.1 M HCl (B_f). The sum ($B_i + B_f$) corresponds to the intracellular iron concentration. All the steps described previously were carried out at 4°C. The concentration of the total iron measured in the first fraction (1.2 mM) was close to that of the second fraction (0.88 mM) and to the theoretical value (1.00 mM), showing the validation of the protocol used.

RESULTS

Fate of FeNTA and NTA during degradation processes. (i) Photodegradation. Figure 3 presents an in situ ^{1}H NMR spectrum of a sample of ABT photodegradation in the presence of FeNTA exposed to light over 50 h. Various signals appeared during the irradiation and can be easily identified as FeNTA, NTA, IDA, glycine, and formate (see Fig. 1 for their chemical structures). The chemical shifts of glycine, NTA, and IDA are pH dependent. Therefore, titration curves had to be plotted (see Materials and Methods) to correctly assign these resonances. These results clearly show that FeNTA was transformed into IDA, glycine, and formate. The same compounds were also observed with a solution of FeNTA under irradiation in the absence of ABT. Figure 4 shows the time courses of the different photoproducts of FeNTA as a function of irradiation time obtained during this experiment. The quantification was carried out after iron precipitation in order to obtain sharp, quantifiable NMR signals. FeNTA clearly disappeared with time, while IDA and glycine accumulated. The formate concentration first increased and then was transformed, likely into CO_2.

(ii) Biodegradation and photobiodegradation. The following experiments (biodegradation and photobiodegradation) of the FeNTA complex (1 mM) or of the NTA ligand (1 mM) were monitored by in situ ^{1}H NMR in a way similar to that described above for photodegradation. Figure 5A and B show the time courses of NTA and IDA concentrations, respectively, under these conditions. The biodegradation of FeNTA by *Rhodococcus rhodochrous* OBT18 led to the formation of IDA. No formation of glycine and only a small and transient amount of formate could be observed. Actually, these two compounds were well biodegraded, as proved by their incubation with this bacterial strain (data not shown), and did not accumulate.

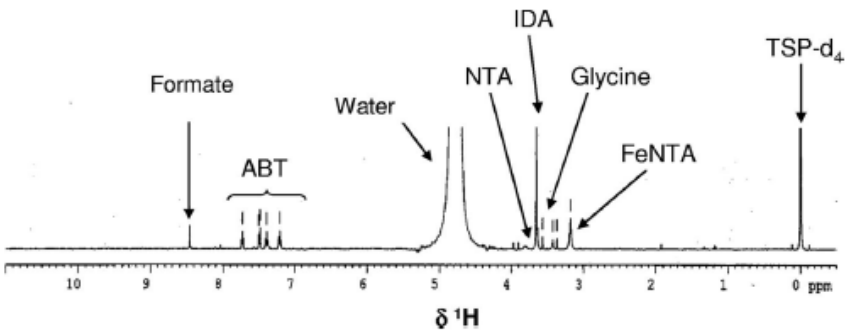

FIG. 3. ^{1}H NMR spectrum of a sample containing ABT and FeNTA collected after 50 h of irradiation. TSP-d_4 is the internal reference.

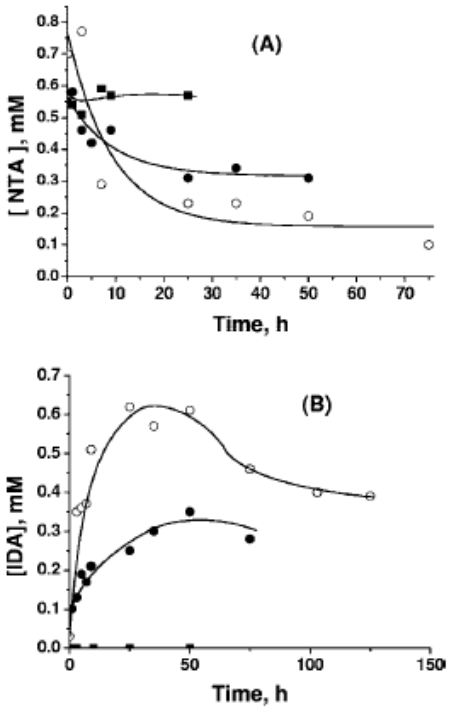

FIG. 5. Incubation of FeNTA (1.0 mM) with *Rhodococcus rhodochrous* OBT18 cells alone (●) or combined with light irradiation (○) and incubation of the ligand NTA without iron with *Rhodococcus rhodochrous* cells alone (■). Time courses of the concentrations of NTA (A) and IDA (B). Concentrations were measured by ^{1}H NMR.

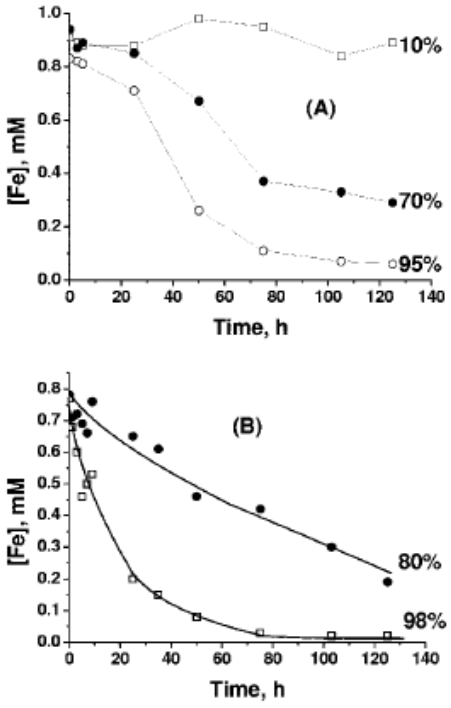

FIG. 6. Time courses of soluble iron measured by complexometry under various conditions. [FeNTA] = 1.0 mM; [ABT] = 0.5 mM. (A) Degradation of ABT in the presence of FeNTA with light (□) and with *Rhodococcus rhodochrous* OBT18 with (○) and without (●) light. (B) Incubation of FeNTA with *Rhodococcus rhodochrous* OBT18 in the absence of ABT with (□) and without light (●).

NTA was converted almost quantitatively into IDA and was transformed very slowly after 25 h (Fig. 5B). The combination of photodegradation and biodegradation processes increased the rate of FeNTA disappearance (Fig. 5A): a larger amount of IDA was formed, and after 50 h, IDA was also transformed (Fig. 5B). When the ligand NTA alone was incubated with *Rhodococcus rhodochrous*, it could not be degraded by the cells (Fig. 5A); no IDA was detected (Fig. 5B).

Fate of iron during degradation processes. Iron was assayed during the degradation processes by complexometric methods under various conditions.

(i) Monitoring of soluble iron under the various processes. Figure 6A presents the results obtained during various degradation processes of ABT in the presence of the FeNTA complex. During the photodegradation process, almost all the soluble iron was maintained at a constant level (only 10% disappearance), whereas it disappeared from the medium during the biodegradation (70%) and photobiodegradation processes (95%). This decrease of the soluble iron concentration in the incubation medium when bacteria were present was confirmed during the incubation of FeNTA alone with cells in the presence or absence of light: 98 and 80% of the iron were removed from the supernatant, respectively (Fig. 6B).

(ii) Localization of the iron. All of these results showed that iron disappeared from the aqueous solution only when cells were present. This prompted us to investigate the localization of iron. A special procedure has been used for the titration of iron in different compartments, i.e., iron in solution, iron at the surface of the cells, and intracellular iron (see Materials and Methods). Iron concentrations were measured in the different compartments after 120 h of incubation by a complexometry technique. If most of the iron was found in solution (0.56 mM), a nonnegligible part was adsorbed at the cell surface (0.13 mM) or was found in the cells (0.19 mM). Therefore, it is clear that part of the iron was transported inside the cells.

DISCUSSION

As reported in this paper, the fate of the FeNTA complex has been investigated under various photodegradation, biodegradation, and photobiodegradation conditions. Studies of the photo- and biodegradation of the ligand NTA and of the iron distribution in cells (extracellular, intracellular, and at the cell surface) helped us to propose mechanisms of photo- and biodegradation of the FeNTA complex.

Proposed mechanism for FeNTA photodegradation. The analysis of ^{1}H NMR spectra collected on samples containing FeNTA exposed to light showed unambiguously the presence of IDA, glycine, and formate. In all cases, formate was further degraded while other photoproducts accumulated. These results show that FeNTA was photodegraded, and a mechanism, based also on previous results obtained with electron paramagnetic resonance measurements (1) in the case of 4-chlorophenol photodegradation, was proposed (Fig. 7). A photoredox mechanism leads (i) to the disappearance of FeNTA with a reduction of Fe(III) to Fe(II) and an oxidation of the ligand

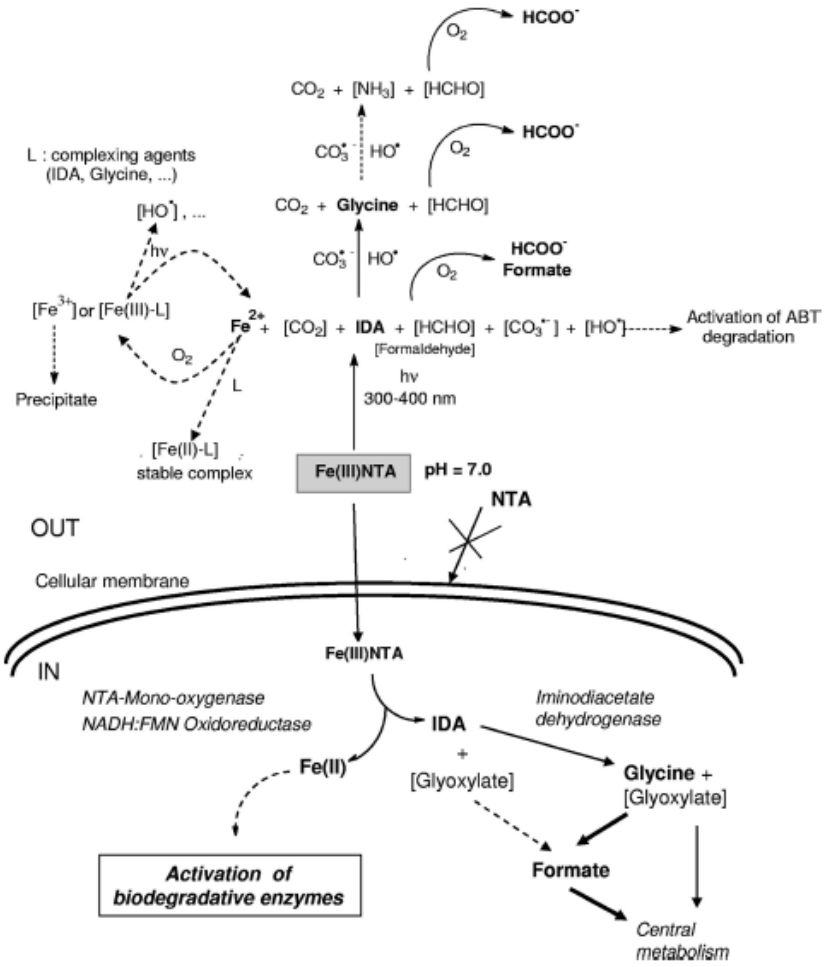

FIG. 7. Proposed mechanisms for FeNTA photodegradation and biodegradation by *Rhodococcus rhodochrous*. All the steps represented by solid line arrows as well as the products written in bold are demonstrated in this work. Dotted line arrows and products in brackets are based on the literature (references 1 and 2 for phototransformation mechanisms and references 4 and 9 for biotransformation mechanisms).

NTA, (ii) to the formation of $HO^{\bullet}$ and $CO_3^{\bullet -}$ radicals, and (iii) to the formation of formaldehyde and IDA. In the present study, formaldehyde could not be detected by ^1H NMR, as its resonance is under the water signal, but formate, its oxidation product, could be observed. The $HO^{\bullet}$ and $CO_3^{\bullet -}$ radicals formed can then react with ABT. The activation of ABT photodegradation could thus be due to the photoinductor effect of FeNTA. Under these photoreaction conditions, most of the iron was maintained in solution. At pH 7.0, this result can be surprising, as (i) Fe(II) is oxidized very fast at this pH with dissolved O_2 present in water and (ii) Fe(III) tends to precipitate if it is not complexed by a ligand. However, in a previous study, stable Fe(II) has been observed between pH 4.0 and 8.0 (1). The presence of Fe(II) at pH 7.0 can be explained by the formation of a stable complex with IDA, the primary product of the photoredox process of FeNTA. Moreover, Fe(III) can also be stabilized by complexation with photoproducts of NTA or of ABT, the starting pollutant. In this case, only a small amount of iron would precipitate.

Proposed mechanism for FeNTA biodegradation by *R. rhodochrous*. The different experiments carried out in this work allowed us to propose a mechanism for the fate of FeNTA in the presence of *Rhodococcus* cells (Fig. 7). The first step corresponds to the entrance of the complex into the cell. The question is whether FeNTA is transported as a complex with iron or as a free form (NTA). The literature does not give any precise answer about the entrance of FeNTA, or of iron and the ligand NTA independently, after FeNTA decomplexation (9). To answer this question, ^1H NMR was used to monitor the fate of FeNTA and the ligand NTA alone during incubations with *Rhodococcus rhodochrous* cells. These bacteria degrade FeNTA into IDA, glycine, and formate, but NTA alone was not degraded. This means that FeNTA is transported inside the cell as a complex because the enzymes known to degrade this compound are intracellular (9). The exact mode of FeNTA transport remains unknown. As a complementary result, assays of iron titration in the different compartments (in solution, at the surface, and inside the cells) showed that iron is partly recovered inside the cells. Based on the metabolic pathways described by Egli (9) and Bucheli-Witschel and Egli (4), the following steps for the degradation of FeNTA in the cell can be proposed (Fig. 7). Intracellular Fe(III) NTA is transformed

into IDA and glyoxylate by an $NADH_2$:FMN oxidoreductase/NTA-monooxygenase labile enzyme complex which simultaneously reduces Fe(III) to Fe(II). The alternative activity of an NTA dehydrogenase can be excluded as it accepts only NTA as a substrate, and we have shown that NTA was not biotransformed by *Rhodococcus* cells. IDA can be further transformed into glycine and glyoxylate by an iminodiacetate dehydrogenase. All of these compounds can enter the central metabolism and end as CO_2. Actually, we could not detect any glyoxylate under our conditions, but instead formate was identified, which could result from the transformation of glyoxylate via oxalate (KEGG, glyoxylate and dicarboxylate metabolism; http://www.genome.jp). It is quite interesting to see the similarity of the reactions between photo- and biodegradation of FeNTA that both lead to Fe(II) and the same intermediates (IDA, glycine, and formate) (Fig. 7).

The question remains as to how FeNTA was able to activate the biodegradation of ABT by *R. rhodochrous* cells observed previously (5). This activation was quite unexpected because no example was reported before, even for other organic compounds in the case of bacteria from the genus *Rhodococcus*. A few studies reported the importance of iron in biodegradation processes: Dinkla et al. (8) showed that iron limitation inhibited the degradation of toluene by two *Pseudomonas putida* strains. Recently, Santos et al. (12) emphasized the stimulation of anthracene biodegradation and surfactant production with other *Pseudomonas* strains by the addition of different forms of soluble iron. Also, the biodegradation of carbazole by a *Sphingomonas* strain immobilized in gellan gum gel beads containing magnetite was reported (16). In our group, we have clearly shown an increase of *Rhodococcus rhodochrous* biodegradation activity of ABT by FeNTA (5). Based on Fig. 7, we could suggest that Fe(II) issued from the intracellular degradation of FeNTA could stimulate the activity of oxidative enzymes such as dioxygenases involved in the biodegradation pathway of ABT. Indeed, it was shown that purified dioxygenases containing a [^{2}Fe-^{2}S] cluster and Fe(II) on different sites could be inhibited when Fe(II) was oxidized in Fe(III) and reactivated by the addition of Fe(II) (6, 13, 15). This phenomenon shown in vitro could occur in vivo in *Rhodococcus* cells. Also, our results are consistent with those of Dinkla et al. (8), who showed that the activities of one monooxygenase and two dioxygenases were increased after the addition of iron to a toluene-degrading *Pseudomonas* strain previously grown on iron-depleted medium. Such enzymes have been shown to be involved in the biodegradation of benzothiazole derivatives (10, 11).

Photo- and biodegradation of the FeNTA complex. In the presence of the FeNTA complex, the biodegradation of ABT was increased and the disappearance kinetics of ABT were very similar with or without light. The main difference between these two conditions was the concentration of soluble iron in the medium. In the presence of light, the disappearance of iron from the solution was faster. To explain this difference, two hypotheses can be proposed based on the fact that the photochemical process leads to the reduction of Fe(III) into Fe(II): (i) Fe(II) could be internalized by the cells more easily than the Fe(III) species and could act directly as an iron source for enzymes, and (ii) at pH 7.0 and in the presence of dissolved oxygen, Fe(II) undergoes a fast oxidative precipitation and, as a consequence, is eliminated from the solution. However, the reoxidation of Fe(II) may produce $Fe(OH)_3$, which is less polymeric and less crystalline than aged Fe(III) hydroxides. This iron species, $Fe(OH)_3$, is more soluble and quicker to approach equilibrium with monomeric Fe(III) species and may be more easily used by the cells. This can explain why no real difference in the rates of disappearance of ABT is found when light is present or absent. It is also interesting to note that the production of radicals resulting from photodegradation processes in the presence of FeNTA did not inhibit biodegradation activity when both light, FeNTA, and microorganisms were combined.

In conclusion, the fate of FeNTA was studied in detail during ABT degradation processes, and mechanisms for the photo- and biodegradation of FeNTA could be proposed. We have shown for the first time that a strain of the genus *Rhodococcus* can degrade FeNTA. This is also the first gram-positive bacterium shown to degrade FeNTA, as previous examples involved gram-negative bacteria (4, 17). This is of primary importance when considering more generally the fate of NTA in the environment, as it suggests the possibility that a wide variety of strains are able to degrade it. A striking feature is the great similarity between the photo- and biodegradation processes of FeNTA: common intermediates were observed, likely because they both involve oxidoreduction mechanisms. Finally the mechanism proposed for FeNTA biodegradation, although it remains highly speculative, suggests that the intracellular iron reduced as Fe(II) could activate enzymes involved in the biodegradation pathway of ABT, and more particularly mono- or dioxygenases.

ACKNOWLEDGMENTS

We thank the French Embassy in Moldova for A.B.'s Ph.D. fellowship and the INTAS for its financial support.

Elodie Cano is gratefully acknowledged for her technical assistance in microbiology.

REFERENCES

1. **Abida, O., G. Mailhot, M. Litter, and M. Bolte.** 2006. Impact of iron-complex (Fe(III)-NTA) on photoinduced degradation of 4-chlorophenol in aqueous solution. Photochem. Photobiol. Sci. **5**:395–402.
2. **Andrianirinaharivelo, S. L., J.-F. Pilichowski, and M. Bolte.** 1993. Nitrilotriacetic acid transformation photo-induced by complexation with iron(III) in aqueous solution. Transition Met. Chem. **18**:37–41.
3. **Besse, P., B. Combourieu, G. Boyse, M. Sancelme, H. De Wever, and A.-M. Delort.** 2001. Long-range ^{1}H-^{15}N heteronuclear shift correlation at natural abundance: a tool to study benzothiazole biodegradation by two *Rhodococcus* strains. Appl. Environ. Microbiol. **67**:1412–1417.
4. **Bucheli-Witschel, M., and T. Egli.** 2001. Environmental fate and microbial degradation of aminopolycarboxylic acids. FEMS Microbiol. Rev. **25**:69–106.
5. **Bunescu, A., P. Besse-Hoggan, M. Sancelme, G. Mailhot, and A.-M. Delort.** 2008. Comparison of microbial and photochemical processes and their combination for degradation of 2-aminobenzothiazole. Appl. Environ. Microbiol. **74**:2976–2984.
6. **Candidus, S., K.-H. Van Pée, and F. Ligens.** 1994. The catechol 2,3-dioxygenase gene of *Rhodococcus rhodochrous* CTM: nucleotide sequence, comparison with isofunctional dioxygenases and evidences for an active-site histidine. Microbiology **140**:321–330.
7. **De Wever, H., S. De Cort, I. Noots, and H. Verachtert.** 1997. Isolation and characterization of *Rhodococcus rhodochrous* for the degradation of the wastewater component 2-hydroxybenzothiazole. Appl. Microbiol. Biotechnol. **47**:458–461.
8. **Dinkla, I. J. T., E. M. Gabor, and D. B. Janssen.** 2001. Effects of iron limitation on degradation of toluene by *Pseudomonas* strains carrying the TOL (pWWO) plasmid. Appl. Environ. Microbiol. **67**:3406–3412.
9. **Egli, T.** 2001. Biodegradation of metal-complexing aminopolycarboxylic acids. J. Biosci. Bioeng. **92**:89–97.
10. **Haroune, N., B. Combourieu, P. Besse, M. Sancelme, T. Reemtsma, A. Kloepfer, A. Diab, J. S. Knapp, S. Baumberg, and A. M. Delort.** 2002.

Benzothiazole degradation by *Rhodococcus pyridinovorans* strain PA: evidence of a catechol 1,2-dioxygenase activity. Appl. Environ. Microbiol. **68:** 6114–6120.

11. **Haroune, N., B. Combourieu, P. Besse, M. Sancelme, A. Kloepfer, T. Reemtsma, H. De Wever, and A. M. Delort.** 2004. Metabolism of 2-mercaptobenzothiazole by *Rhodococcus rhodochrous.* Appl. Environ. Microbiol. **70:** 6315–6319.
12. **Santos, E. C., R. J. S. Jacques, F. M. Bento, M. C. R. Peralba, P. A. Selbach, E. L. S. Sà, and F. A. O. Camargo.** 2008. Anthracene biodegradation and surface activity by an iron-stimulated *Pseudomonas* sp. Bioresour. Technol. **99:**2644–2649.
13. **Schach, S., B. Tshisuaka, S. Fetzner, and F. Ligens.** 1995. Quinoline 2-oxidoreductase and 2-oxo-1,2-dihydroquinoline 5,6-dioxygenase from *Comamonas testosteroni* 63. The first two enzymes in quinoline and 3-methylquinoline degradation. Eur. J. Biochem. **232:**536–544.
14. **Stookey, L. L.** 1970. Ferrozine—a new spectrophotometric reagent for iron. Anal. Chem. **42:**779–781.
15. **Wackett, L. P., L. D. Kwart, and D. T. Gibson.** 1988. Benzylic monooxygenation catalyzed by toluene dioxygenase from *Pseudomonas putida.* Biochemistry **27:**1360–1367.
16. **Wang, X., Z. Gai, B. Yu, J. Feng, C. Xu, Y. Yuan, Z. Lin, and P. Xu.** 2007. Degradation of carbazole by microbial cells immobilized in magnetic gellan gum gel beads. Appl. Environ. Microbiol. **73:**6421–6428.
17. **Yuan, Z., and J. M. VanBriesen.** 2008. Bacterial growth on EDTA, NTA and their biodegradation intermediates. Biodegradation **19:**41–52.